Journal of Applied Electrochemistry **29**: 411–419, 1999.

Electrochemical reduction of chromate ions from dilute artificial solutions in a GBC-reactor

K. N. NJAU and L. J. J. JANSSEN
Eindhoven University of Technology, Department of Chemical Engineering, Laboratory of Instrumental Analysis, PO Box 513, 5600 MB Eindhoven, The Netherlands

Received 6 February 1998; accepted in revised form 6 September 1998

Key words: chromate, gas diffusion electrode, heavy metals, mass transfer, packed bed electrode

Abstract

Reduction of chromate in very low concentration (20 ppm) has been carried out in a GBC reactor. Final concentrations below 0.5 ppm have been achieved at reasonable reaction rates. Spontaneous reduction of chromate by hydrogen in a GBC reactor without an external power source requires careful selection of cathode material. Chemically stable materials such as titanium and RVC tend to passivate when in contact with chromate solution and are unsuitable for use as cathode materials. Graphite, active carbon and graphite felt show no obvious passivation. Reduction of oxidized groups and oxygen are the major side reactions. These occur significantly, especially when using an activated carbon bed as a cathode.

List of symbols

a_e	specific surface area of bed (m^{-1})
A_b	surface area of bed (m^2)
A_e	effective electrode area of bed (m^2)
A_g	geometric surface area of gas diffusion electrode (m^2)
C_{HS}	concentration of sulfuric acid ($mol\ m^{-3}$)
C_r	concentration of chromate in reactor ($mol\ m^{-3}$)
C_v	concentration of chromate in reservoir ($mol\ m^{-3}$)
$C_{v,o}$	initial concentration of chromate in reservoir ($mol\ m^{-3}$)
D_{Cr}	diffusion coefficient for chromate ion ($m^2\ s^{-1}$)
D_{Fe}	diffusion coefficient for ferric ion ($m^2\ s^{-1}$)
D_{ox}	diffusion coefficient for oxygen ion ($m^2\ s^{-1}$)
F	Faraday's constant (96 487 $C\ mol^{-1}$)
i	current density ($A\ m^{-2}$); $i = I/A_g$
i_{Cr}	chromate current density ($A\ m^{-2}$)
i_T	total current density ($A\ m^{-2}$)
I	current (A)
I_{Cr}	chromate current (A)
I_T	total current (A)
k	electrochemical rate constant ($m\ s^{-1}$)
k_{ch}	chemical rate constant ($m\ s^{-1}$)
k_m	mass transfer coefficient ($m\ s^{-1}$)
$k_{m,Cr}$	mass transfer coefficient for chromate ion ($m\ s^{-1}$)
$k_{m,ox}$	mass transfer coefficient for oxygen ($m\ s^{-1}$)
k_{ov}	overall rate constant ($m^3\ s^{-1}$); $k_{ov} = kA_e$
$k_{ov,ch}$	overall chemical rate constant ($m^3\ s^{-1}$); $k_{ov,ch} = k_{ch}A_b$
$k_{ov,no}$	overall rate constant without oxygen purging ($m^3\ s^{-1}$)
$k_{ov,ox}$	overall rate constant with oxygen purging ($m^3\ s^{-1}$)
K	constant with value of 1 ($mol^{1-\alpha}\ m^{3\alpha-3}$)
n	number of electrons involved in electrode reaction (dimensionless)
r_{Cr}	reaction rate ($mol\ s^{-1}$)
t	time (s)
T	temperature (K)
Q_s	volumetric flow rate of solution ($m^3\ s^{-1}$)
u_s	mean velocity of solution ($m\ s^{-1}$)
V_r	reactor volume (m^3)
V_s	volume of solution (m^3)
V_v	volume of solution in reservoir (m^3)

Greek symbols

α	apparent order of reaction
ϵ_b	bed voidage
τ_v	solution residence time in reservoir(s); $\tau_v = V_v/Q_s$
τ_r	solution residence time in reactor(s); $\tau_r = \epsilon_b V_r/Q_s$

1. Introduction

Hexavalent chromium has received increased attention because of its toxic nature. Waste water polluted with hexavalent chromium results from sources such as the textile, metal finishing, pigment, drug and organic chemical industries, and from cooling systems where hexavalent chromium is added as a corrosion inhibitor [1, 2]. Several procedures have been suggested for the treatment of waste solutions containing chromium.

Some processes based on electrochemistry have been proposed, such as the use of a three dimensional cathode to reduce chromate, a rotating cylinder cell [1, 2] and, most recently, the combination of a hydrogen gas diffusion anode and a three-dimensional cathode [3–5] to form the GBC reactor. The application of a three-dimensional cathode has been particularly useful in treating solutions with a low chromate concentration to improve the productivity of a commercial system and therefore meet the operation costs on a realistic level [6].

Chromium can be captured electrochemically as a nonsoluble ionic compound such as $Cr(OH)_3$ [2, 7]. Chromate can also first be electrochemically reduced to Cr(III) ions which can later be precipitated as $Cr(OH)_3$ [3]. The electrochemical reduction of chromate ions may also give rise to the formation of poorly soluble compounds on the electrode. It is reported that, in the absence of foreign ions, chromic acid can only be reduced at graphite and gold electrodes [8].

The use of the GBC for the reduction of chromate is reported in [3]. This is a reactor which combines a porous cathode and a gas diffusion electrode to reduce chromate ions without the need for an external power source. The working principle of this type of reactor has been described earlier [3–5].

Several studies have been reported on the kinetics of the electrochemical reduction of hexavalent chromium and have shown that the reduction products depend on the acidity of the solution. Most of these studies have shown that the final product is usually a Cr^{3+} compound and the electro-deposition of chromium metal from divalent and trivalent chromium salts from strongly acidic solutions below pH 1.8 is impossible [1]. Deposition of chromium metal from Cr^{6+} solutions is possible only within certain limits of the CrO_3/SO_4^{2-} ratio which ranges from 18.2 to 127.5; beyond these limits deposition of chromium metal is not possible [9].

The aim of this work is to investigate the reduction of chromate in low concentrations ($\sim$20 ppm Cr^{6+}) in acidic solutions with a GBC reactor. In industrial process waters such low chromate concentrations are quite normal. The amount of Cr^{6+} tolerable for the environment is in the ppb range, hence the decision to work with low concentrations in this study [10]. The influence of solution properties and the cathode material on reduction kinetics as well as the contribution of side reactions are investigated.

2. Theory

The working principle of GBC reactor has been described in [5]. A procedure is proposed for treating batch recycle data to fit the macroscopic equation

$$-r_{Cr} = KkA_e C_r^{\alpha} = Kk_{ov} C_r^{\alpha} \quad (1)$$

where K is an arbitrary constant with a value of 1 and dimensions $mol^{(1-\alpha)}\ m^{(3\alpha-3)}$. The actual electrode area A_e depends on the active bed thickness and is not necessarily equivalent to the total electrode area A_b. The overall rate constant $k_{ov} = kA_e$ governs the GBC reactor performance during chromate reduction. When the system is diffusion controlled, k is essentially the mass transfer coefficient k_m and can be predicted using mass transfer correlation equations.

For a batch recycle system with a low conversions per pass, the system can be described as a continuous stirred tank electrochemical reactor (CSTER), and a non steady mass-balance equation can be obtained [5],

$$\ln\left(\frac{1}{\tau_r}(C_v - C_r) - \frac{dC_r}{dt}\right) = \ln\left(\frac{KA_e k}{\epsilon_b V_r}\right) + \alpha \ln(C_r) \quad (2)$$

The chromate concentration in the reactor C_r is calculated from an equation obtained from the mass balance describing changes in the reservoir, namely,

$$\frac{dC_v}{dt} = \frac{1}{\tau_v}(C_r - C_v) \quad (3)$$

For reactor residence times $\tau_r \ll 5$ s dC_r/dt is less than 2% of $(C_v - C_r)/\tau_r$ and therefore the term dC_r/dt in Equation 2 can be neglected. This, in combination with Equation 3, simplifies Equation 2 to

$$\ln\left(-\frac{dC_v}{dt}\right) = \ln\left(\frac{Kk_{ov}}{V_v}\right) + \alpha \ln C_r \quad (4)$$

This implies that the order and the overall rate constant k_{ov} may be obtained from the concentration–time data for the reservoir. The procedure adopted is similar to that in [5]. The chromate ion concentration in the reservoir is monitored at discrete time intervals, then dC_v/dt is calculated at discrete time intervals using a three-point differentiation formula. During a batch

recycle operation with a divided cell both the current across the cell and the concentration of the electroactive species can be followed during the experiment. The chromate current is related to the reaction rate in the reactor by

$$I_{Cr} = n\,Fr_{Cr} \tag{5}$$

3. Experimental details

The experimental set-up was a batch recycle system consisting of a laboratory scale cell, a 3 dm^3 glass reservoir, a pump, a flow meter and a heat exchanger. A schematic representation of the cell is shown in Figure 1. Five types of material were used for the cathode, namely a bed of graphite particles of sizes between 1–2 mm and irregular shapes, a bed of active carbon particles (NORIT), cylindrical in shape with a diameter of 1 mm and an average length of 3 mm, a block of RVC (ElectroCell AB) with a porosity of 97 and 100 pores per inch (ppi), a stack of expanded titanium sheets and a piece of graphite felt. The cathode chamber was 1.8 cm thick, 2.7 cm high and 2.6 cm wide. The cathode filled the whole cathode chamber. A graphite plate approximately 5 mm thick was used as the cathode current feeder.

The anode was an E-TEK Elat Vulcan GDE with dimensions of 2.0 cm × 2.0 cm and one side was covered by a Nafion® 117 layer. The catalyst loading of the GDE was 0.4 mg cm^{-2} platinum. The GDE was supported by a perforated platinum plate placed on the gas side as a current collector and to enhance mechanical stability. A platinum foil of about 0.5 mm thick was used as anode current collector. Before each run nitrogen gas was purged through the solution in the reservoir and through the gas compartment of the cell to protect the GDE from reaction with hydrogen and oxygen inside the electrode. The gas diffusion electrode was thereafter fed with pure hydrogen from a gas cylinder; a nitrogen purge in the reservoir was maintained during the experiments.

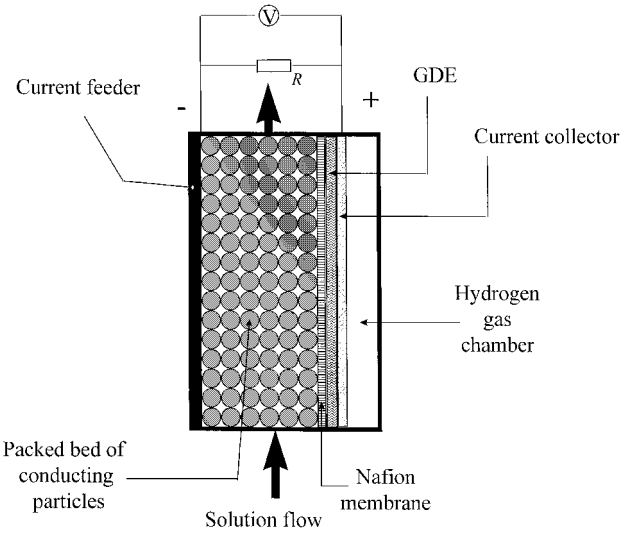

Fig. 1. Schematic representation of GBC reactor.

The electrodes were short-circuited via an external resistance. The potential drop across this resistance was continuously recorded during the experiments and was used to calculate the current flowing through the circuit. The current densities were calculated based on the geometric surface area of the GDE. Table 1 shows the standard conditions of experimentation.

Laboratory solutions were made of potassium dichromate (Merck p.a) in 1 M H_2SO_4. Millipore water was used to make up the solutions. Determination of chromate ion concentration was carried out using an ultraviolet spectrophotometer type Ultrospec II (LKB Biochrom) at a wavelength of 350 nm. The initial chromate concentration was 0.4 mol m^{-3} (20 ppm), the temperature was varied between 298 and 332 K, the H_2SO_4, the molarity between 100 and 1000 mol m^{-3} and the solution flowrate between 6.02×10^{-6} and 1.6×10^{-5} $m^3 s^{-1}$. The initial volume of solution was 3.00 dm^3. The volume of a sample was 5 cm^3 and sampling was carried out every 10 min.

4. Results

4.1. *Effect of the materials of the three-dimensional cathode*

4.1.1. *Packed bed of graphite particles*

The current and the chromate concentration were followed as a function of time during chromate reduction on a graphite bed electrode. Standard conditions were applied. The total current was measured during the experiment while the chromate current I_{Cr} was calcu-

Table 1. Standard parameters

Parameter	Data
Flowrate of solution	1.58×10^{-5} $m^3 s^{-1}$
Temperature	298 K
Initial CrO_4^{2-} concentration	0.4 mol m^{-3} (20 ppm)
H_2SO_4 concentration	1 M
Cathode material	graphite particles (1 mm < d < 2 mm)
Cathode thickness	1.8 mm

lated from the conversion measurements using Equation 5 where $n = 3$ for the reduction of chromate ion to Cr^{3+}. The plots of current density for chromate $i_{Cr} = I_{Cr}/A_g$ and the total current density $i_T = I_T/A_g$ as a function of time are shown in Figure 2. It can be seen that the two current densities are very close to one another and both decline steadily with time. It can also be seen that a maximum current density of about $375\,A\,m^{-2}$ was observed and towards the end of the experiment the current density was very low (about $10\,A\,m^{-2}$).

4.1.2. *Packed bed of active carbon particles*

The same procedure was applied as in Section 4.1.1. The plots of the current density for chromate reduction i_{Cr} and the total current density i_T as a function of time are shown in Figure 3. The chromate current density declines steadily with time, while the total current density increases in the first 600 s from about 313 to a maximum of about $463\,A\,m^{-2}$, thereafter remaining almost constant for 600 s and then declining steadily to $275\,A\,m^{-2}$ at the end of the experiment. There is a very big difference between i_T and i_{Cr} throughout the experiment, caused by a reduction of oxidised groups present on the large surface of the active carbon particles and oxygen present in the solution despite nitrogen gas bubbling through the solution in the reservoir. Since the potential of the cathode must be more positive than the reversible potential of the $H_2 = 2\,H^+ + 2\,e^-$ redox couple, reduction of chromate to chromium metal is not possible.

4.1.3. *Reticulated vitreous carbon*

Reduction of a standard solution of chromate on RVC was carried out without chromate concentration measurements. The total reduction current was followed with time. The results of total current density–time measurements are shown in Figure 4. Initially a very low current density of about $0.5\,A\,m^{-2}$ was obtained.

4.1.4. *Stack of expanded titanium mesh*

A similar experiment to that in Section 4.1.3. was conducted using a stack of expanded titanium meshes. The results of the total current density–time data are also shown in Figure 4, which shows that very low current densities were also encountered during the reduction process.

4.1.5. *Graphite felt*

Similar experiments to those in Section 4.1.3. and Stack of expanded titanium mesh were conducted using graphite felt. The total current density–time data are shown in Figure 5. Current densities i_T comparable to

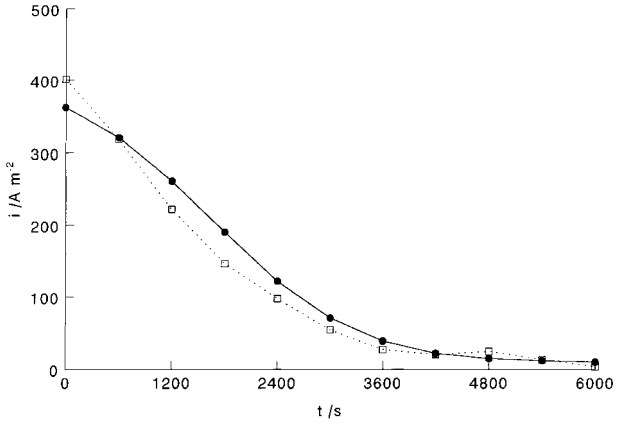

Fig. 2. Total i_T (•) and chromium i_{Cr} (□) current densities as a function of time for a bed of graphite particles at 25 °C.

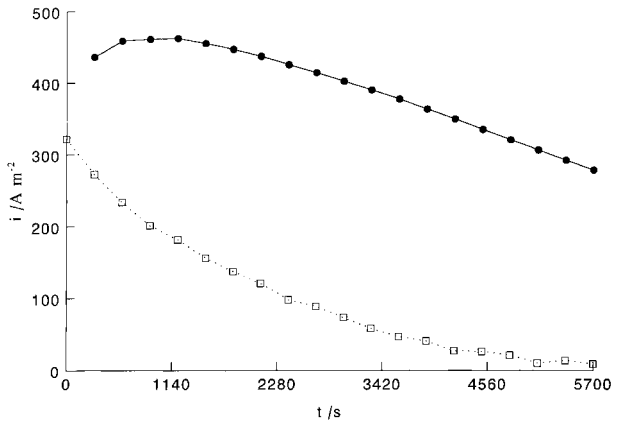

Fig. 3. Total i_T (•) and chromium i_{Cr}(□) current densities as a function of time for a bed of active carbon particles.

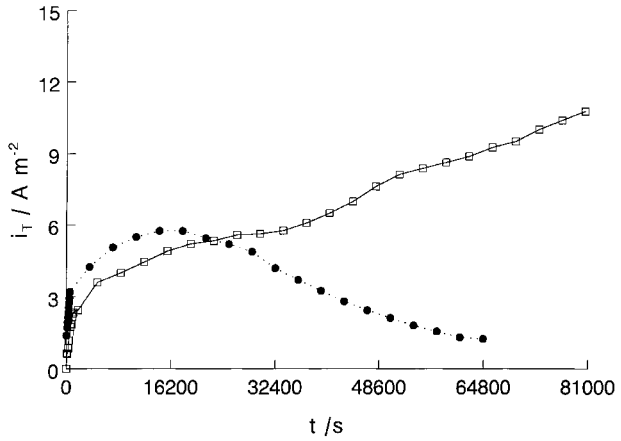

Fig. 4. Total reduction current density for RVC (□) and a stack of expanded titanium mesh (•) as a function of time.

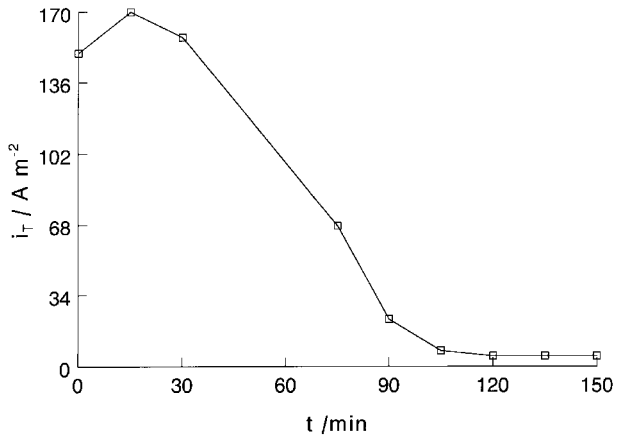

Fig. 5. Total reduction current density as a function of time for graphite felt.

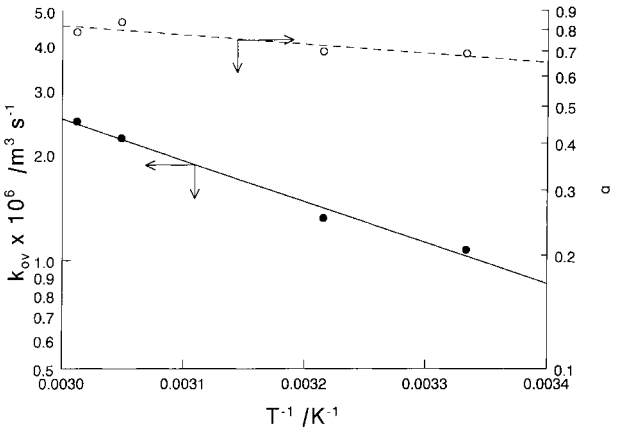

Fig. 7. Log k_{ov} and log α as a function of T^{-1}.

those obtained during chromate reduction on graphite material are observed, although slightly lower. To check whether the electrode had been passivated after the first run, the concentration of chromate was increased from about 0.02 mM to about 1 mM. The experiment was continued and the current density increased to 283 A m^{-2}.

4.2. *Effect of solution properties*

4.2.1. *Temperature*

The effect of temperature on the electrochemical reduction of chromate on a graphite bed cathode was investigated. The temperature was varied from 298 to 332 K. The chromate concentration – time data were used to calculate the α and k_{ov} using Equations 3 and 4. Figure 6 shows a typical $\log(-dC_v/dt)$ against $\log C_r$ curve.

The values of the order α and the apparent rate constant k_{ov} at different temperatures are plotted against T^{-1} in Figure 7. The apparent order α increases from 0.68 to 0.84 and k_{ov} increases from 1.07×10^{-6} to 2.96×10^{-6} m^3 s^{-1}, with temperature increasing from 298 to 332 K. It can also be deduced from the log k_{ov} against $1/T$ curve that the activation energy for the overall process is 22.1 kJ mol^{-1}.

4.2.2. *Solution flowrate*

The effect of solution flowrate on the rate parameters α and k_{ov} is shown in Figure 8, where it can be seen that the effect of the flowrate on α and k_{ov} is relatively low. The slope of the log k_{ov} against log Q_s curve was 0.18.

In a separate experiment where the packed bed was replaced by a flat graphite plate, chromate solution containing 5 mol m^{-3} CrO_4^{2-} ions was reduced at different flowrates. The flowrate was varied within short time intervals so as to minimize the changes in CrO_4^{2-} ion

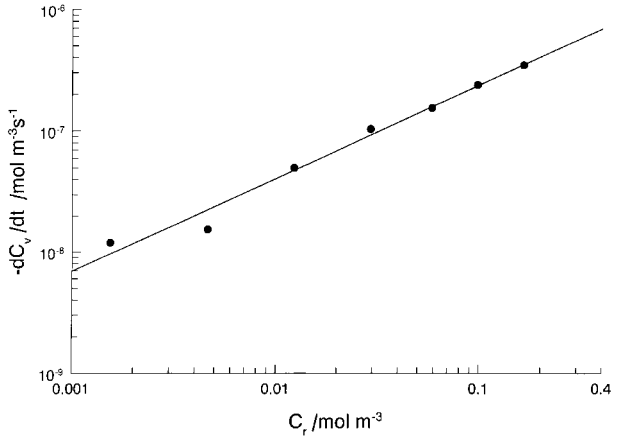

Fig. 6. Log $(-dC_v/dt)$ is plotted against log C_r for chromate reduction on a graphite bed under standard conditions.

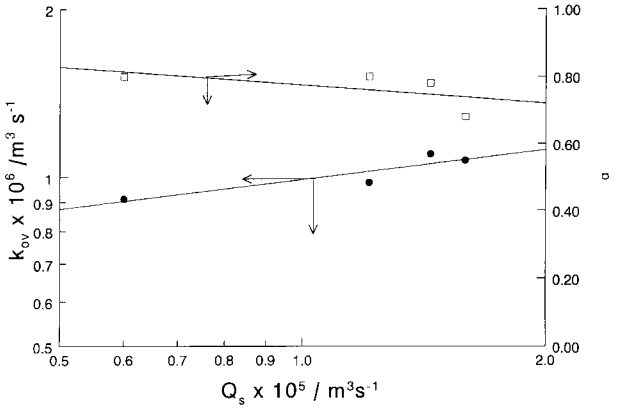

Fig. 8. Overall rate constant, k_{ov}, and order of reaction, α, as a function of solution volumetric flowrate, Q_s.

concentration. The reduction current was monitored and was used to calculate the reduction rate. The calculated rate was plotted against the flowrate in Figure 9 where it is seen that the rate increased by 9% from 3.4×10^{-4} to 3.6×10^{-4} mol m^{-2} s^{-1} when the flowrate was increased from 5×10^{-3} to 50×10^{-3} m^3 s^{-1}. Moreover, it can be seen that above 20×10^{-3} m^3 s^{-1}, the rate was practically constant. The results of this experiment have confirmed that the influence of flowrate during the reduction of chromate in a GBC is small.

4.2.3. *Sulfuric acid concentration*

The sulfuric acid concentration was varied from 0.1 to 1 M, all the other conditions being kept standard. The effect of the sulfuric acid concentration on the reaction rate parameters is shown in Figure 10 where it can be seen that the overall rate constant and the order increase steadily with increasing sulfuric acid concentration.

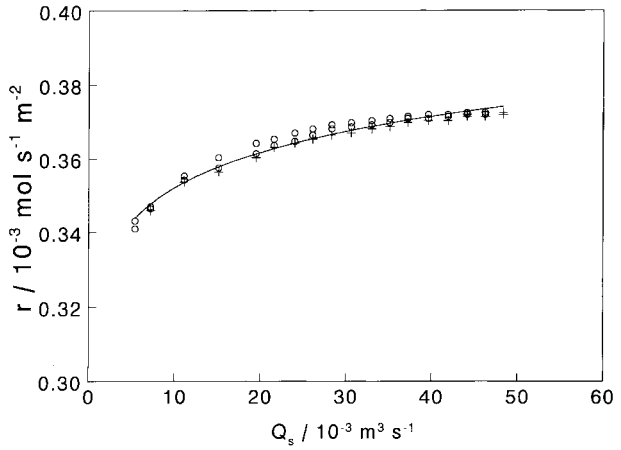

Fig. 9. Reaction rate as a function of flowrate in a GBC reactor with a graphite plate cathode. CrO_4^{2-} concentration: 5 mol m^{-3}, (+) increasing and (○) decreasing the flow.

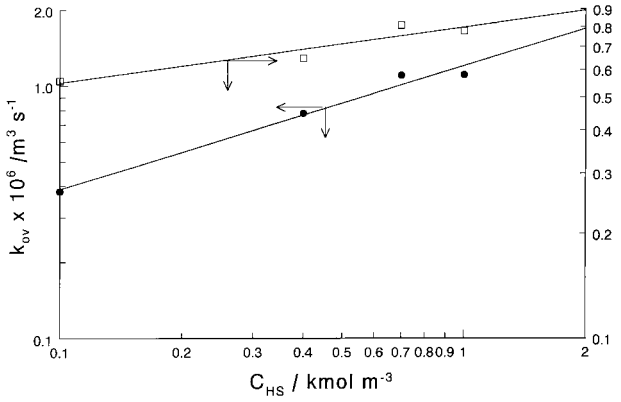

Fig. 10. Overall rate constant, k_{ov}, and order of reaction, α, as a function of H_2SO_4 acid concentration.

4.3. *Ageing effect of the packed bed*

The effect of changes in the behaviour of the active carbon bed with time was investigated by carrying out successive runs with hydrogen gas feed to the GDE. Standard conditions were used. The results of the log C_v against time for a run with nitrogen feed to the GDE and thereafter two consecutive runs with hydrogen feed are shown in Figure 11 showing a clear ageing effect. Moreover, it was found in [3] that the rate constant for chromate reduction by carbon decreases strongly with ageing of the carbon particles. This means that the rate of chromate reduction by carbon decreases during the series of experiments and an accurate correction for the chromate reduction by carbon cannot be carried out for the experiments with hydrogen. It can also be seen that, with a fresh bed, the rate parameters are determined mainly by the chemical reduction of chromate by the active carbon particles.

4.4. *Direct reduction of chromate by the cathode material*

4.4.1. *Reduction of chromate by graphite bed*

Chemical reduction of chromate by a bed of graphite particles in a GBC reactor with nitrogen gas as feed for the GDE was investigated. Standard conditions were maintained. Samples were taken and analysed to determine the decrease in chromate concentration. It was observed that the conversion after 2.5 h was only 1.5%.

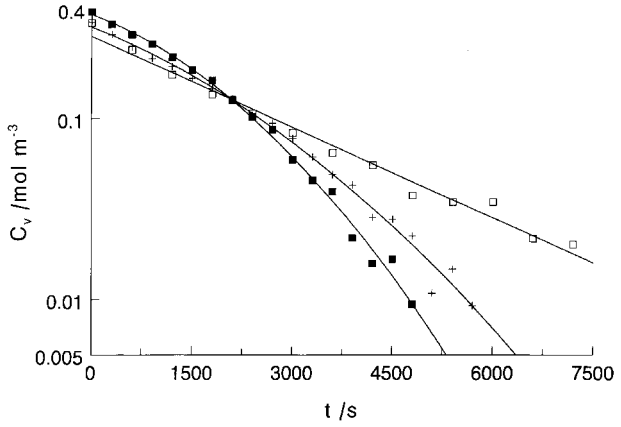

Fig. 11. Ageing effect of the active carbon bed: (□) run 1, N_2 gas feed to the GDE, (+) run 2, H_2 gas feed to the GDE, (■) run 3, H_2 gas feed to the GDE.

4.4.2. *Chromate reduction on an active carbon bed*
Chemical reduction of chromate on a bed of active carbon was investigated by maintaining a stream of nitrogen gas over the GDE. All the other conditions were maintained. In Figure 11 the results for successive experiments are represented; the first was carried out with nitrogen gas as feed for the GDE and the others were carried out using hydrogen gas. Figure 11 indicates a linear relationship between log C_v and t with nitrogen feed. This means that $\alpha = 1$ for chromate reduction by active carbon. The overall chemical rate constant $k_{ov,ch} = 1.24 \times 10^{-6}\,m^3 s^{-1}$ has been deduced from the slope of the straight line from Figure 11.

4.5. *Oxygen reduction*

Reduction of a 1 M H_2SO_4 solution without chromate, but initially saturated with air, on a bed of active carbon was investigated with hydrogen gas feed for the GDE. The reduction current was followed as a function of time. No gas bubbling through the solution was carried out during this experiment. The log I_T against time data are shown in Figure 12, which shows a linear decrease with time t, and therefore $\alpha = 1$. Moreover, from this figure and using Equations 1 and 5, it may be deduced that the rate constant for oxygen reduction $k_{ov,no} = 9.51 \times 10^{-7}\,m^3 s^{-1}$. Using a $KMnO_4$ solution as a titrant, it was found that a small quantity of H_2O_2 was present in the solution after the experiment.

In another experiment, oxygen was continuously purged through 1 M sulfuric acid solution in the reservoir. Samples were analysed for hydrogen peroxide. It was found that the concentration of hydrogen peroxide reaches a limit of $1.5\,mol\,m^{-3}$ within about 2 h. The current efficiency for the production of hydrogen peroxide during the experiment was 2.2%. The results of log I against time are also shown in Figure 12, and show that a steady current of 0.29 A is reached.

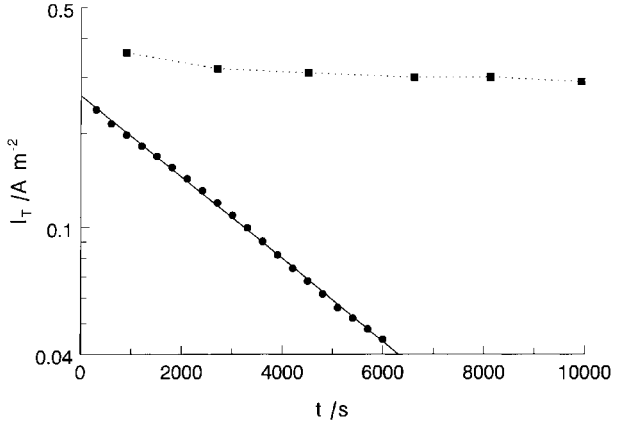

Fig. 12. Reduction of oxygen on an active carbon bed: (■) with oxygen bubbling (●) no gas bubbling.

5. Discussion

5.1. *Mass transfer coefficient for chromate ion*

The mass transfer coefficient for chromate $k_{m,Cr}$ under standard conditions, but for the bed of active carbon particles was calculated from the known data for Fe^{3+} [11]. In Section 2, it was shown that for $u_s > 0.05\,m\,s^{-1}$ the mass transfer coefficient for Fe^{3+} ions is related to the mean flow velocity [11] by

$$k_{m,Fe} = 8.5 \times 10^{-4} u_s^{0.80} \tag{6}$$

In terms of dimensionless numbers in this flow region this becomes

$$Sh = \frac{k_m d_p}{D} = a\,Re^{0.8} Sc^{1/3} \tag{7}$$

where a is a constant.

Substituting parameters for ferric and chromate ions in Equation 10, it can be shown that

$$k_{m,Cr} = \left(\frac{D_{Cr}}{D_{Fe}}\right)^{2/3} k_{m,Fe} \tag{8}$$

The diffusion coefficients for Fe^{3+} and chromate in 1 M H_2SO_4 at 25 °C are reported to be $4.86 \times 10^{-10}\,m^2\,s^{-1}$ [11] and $9 \times 10^{-10}\,m^2\,s^{-1}$ [12], respectively. The mean solution velocity, u_s, in the GBC reactor was calculated from the cross-sectional area of the reactor and bed voidage $\epsilon_b = 0.4$, and was found to be $8.44 \times 10^{-2}\,m\,s^{-1}$.

The mass transfer coefficient $k_{m,Fe}$ at $u_s = 8.44 \times 10^{-2}\,m\,s^{-1}$ was then calculated from Equation 11 and found to be $1.17 \times 10^{-4}\,m\,s^{-1}$. The mass transfer coefficient for chromate $k_{m,Cr,}$ under standard conditions is therefore $1.76 \times 10^{-4}\,m\,s^{-1}$. The value of $k_{m,Cr}\,A_b$ can be calculated from the volume of the reactor and the specific bed electrode area $a_e = 2800\,m^{-1}$ [11] which has been calculated from the external surface of the particles, assuming that the internal surface of the carbon particles does not take part in the reduction of chromate. The value $k_{m,Cr}A_b$ was found to be $6.23 \times 10^{-6}\,m^3\,s^{-1}$.

5.2. *Three-dimensional electrode material*

From Section 4.1.1. follows that the electrochemical reduction of chromate from dilute acidic solutions using GBC reactor fed with hydrogen is highly dependent on

the type of cathode substrate. Inhibition of the electrode surface during electrochemical reduction of chromate has been reported for gold and platinum electrodes [12]. It was noted in [12] that during a positive potential sweep in rotating disc electrode (RDE) experiments, clear inhibition is observed. The more chemically stable carbon materials, such as RVC, and noncarbon materials, such as titanium, show a high degree of passivation during chromate reduction. This passivation has been attributed to the formation of stable inhibiting compounds on the surface of the cathode which remain well attached to the cathode surface.

The good performance of the less stable carbon cathodes, such as graphite, active carbon and graphite felt may be the result of the occurrence of a direct chromate reduction on the oxide-free surfaces of carbon to form carbon oxides. A fresh active carbon bed shows the highest reactivity to the chemical chromate reduction while graphite materials show weak reactivity. It is possible that the reduction of oxidised groups on carbon takes place and thereafter re-oxidation by chromate occurs in which Cr(III) is formed. It is suggested that the direct reaction of chromate with carbon substrate refreshes the surface of the cathode, and part of the carbon surface remains active to electroreduction of chromate. Although this behaviour seems to be of advantage, it must be pointed out that the reduction of chromate by the substrate consumes the electrode material and thus reduces the bed compactness, a situation which can, significantly decrease the overall conversion over the reactor [11] due to poor electrical contact. The reaction of carbon with chromate for active carbon has been observed in Section 4.2.2 to proceed at a rate constant $k_{ov,ch} = 1.24 \times 10^{-6}\,m^3\,s^{-1}$, which is five times lower than the value of $k_{m,Cr}\,A_b$, which is $6.23 \times 10^{-6}\,m^3\,s^{-1}$ (Section 5.1). This means that the chemical reduction of chromate is also determined by kinetic parameters.

5.3. *Spontaneous reduction of chromate by hydrogen*

Despite the low chromate concentration, chromate reduction in a GBC reactor is influenced by both electrochemical and diffusion processes. In all conditions tested, a value of the order $\alpha < 1$ was observed. Low final concentrations (< 0.5 ppm) were obtained in relatively short experimental times, that is, between 1 and 2 h, depending on the conditions of the experiment.

There is an increase of α with increasing temperature indicating an increasing influence of the diffusion process. An activation energy of $22.1\,kJ\,mol^{-1}$ was obtained from the plots of $\log k_{ov}$ against T^{-1}, showing a process that is highly influenced by mass transfer. In these experiments the influence of solution conductivity on α and k_{ov} as shown in Figure 10, is less significant because of the low current through the reactor.

As shown in Equation 7, k_{ov} is proportional to $Q_s^{0.18}$. The exponent 0.18 is much lower than would be expected for a pure mass transfer coefficient k_m, which would be between 0.45 and 0.8 in the flow regime used [13]. This means that kinetic parameters of electroreduction also affect the rate of chromate reduction.

5.4. *Oxygen reduction*

Oxygen reduction by hydrogen is the major side reaction during reduction of chromate on active carbon particles. The diffusion coefficient for oxygen in 1 M H_2SO_4 and 25 °C is $2.02 \times 10^{-9}\,m^2\,s^{-1}$ [15]. Similarly to the calculation of $k_{m,Cr}$, the mass transfer coefficient of oxygen in 1 M H_2SO_4 was found to be $3.03 \times 10^{-4}\,m\,s^{-1}$ and $k_{m,ox}A_b$ was $1.07 \times 10^{-5}\,m^3\,s^{-1}$. From the slope of the $\log I_T$ against t curve in Figure 12, the overall rate constant for oxygen reduction in the experiment without gas bubbling $k_{ov,no}$ was found to be $9.51 \times 10^{-7}\,m^3\,s^{-1}$. The steady current obtained during the experiment with oxygen bubbling was 0.29 A. The overall rate constant for oxygen reduction during the experiment with oxygen bubbling was calculated using $I_{ox} = 4\,F\,k_{ov,ox}\,C_{ox}$ and the solubility of oxygen in 1 H_2SO_4, namely, $1.01\,mol\,m^{-3}$ [14]. It was found that the overall rate constant for oxygen reduction $k_{ov,ox} = 7.45 \times 10^{-7}\,m^3\,s^{-1}$. Both values of k_{ov} for oxygen reduction are practically the same. From this it is concluded that dissolved oxygen is reduced in both cases and that oxygen reduction on active carbon particles is kinetically controlled.

6. Conclusion

The reduction of chromate in a GBC reactor can be carried out to a very low chromate concentration, namely below 0.5 ppm. Spontaneous reduction of chromate by hydrogen in a GBC reactor requires a careful selection of bed material. Graphite, active carbon and graphite felt have shown good results while the more chemically stable materials, namely expanded titanium and RVC, are unsuitable as cathode materials.

References

1. A. Radwan, A. El-Kiar, H.A. Farag and G.H. Sedahmed, *J. Appl. Electrochem.* **22** (1992) 1161.
2. D. Golub and Y. Oren, *J. Appl. Electrochem.* **19** (1989) 311.

3. E.C.W. Wijnbelt and L.J.J. Janssen, *J. Appl. Electrochem.* **24** (1994) 1028.
4. L.J.J. Janssen, *Netherlands Patent* 9 101 022 (1991).
5. I. Portegies Zwart and L.J.J. Janssen, *J. Appl. Electrochem.* **28** (1998) 1.
6. L. Lipp and D. Pletcher, *Electrochim. Acta* **42** (1997) 1101.
7. I.C. Agarwal, A.M. Rochon, H.D. Geser and A.B. Sparling, *Water Res.* **18** (1984) 227.
8. F.I. Danilov and M.N. Ben-Ali, *Elektokhimiya* **24** (1988) 54.
9. G. Isserlis, *in* 'Industrial Electrochemical Processes', edited by A.T. Kuhn (Elsevier, New York, 1971).
10. International Standards for Drinking Water 3rd edn (WHO, Geneva 1971).
11. K. Njau, W.-J. van der Knaap and L.J.J. Janssen, *J. Appl. Electrochem.* **28** (1998) 343.
12. L.D. Burke and P.F. Nugent, *Electrochim. Acta* **42** (1997) 399.
13. D. Genders, *in* 'Electrochemistry for a Cleaner Environment', edited by N. Weinberg (The Electrosynthesis Company, 1992).
14. IUPAC, 'Solubility Data Series Vol 7: Oxygen and Ozone' (Pergamon Press, Oxford, 1981).
15. J.J. Lingane, *J. Electroanal. Chem.* **2** (1961) 296.